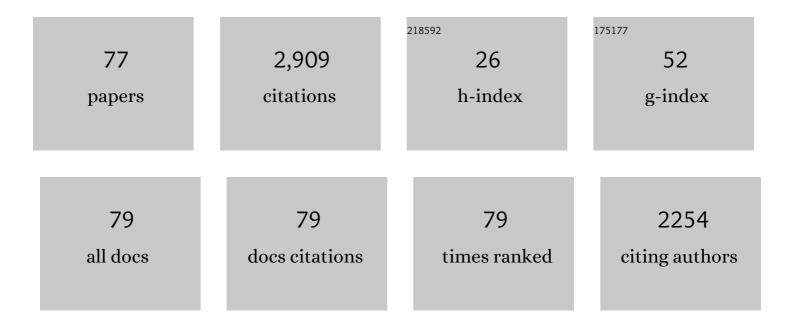
Lukas P Baumgartner

List of Publications by Year in descending order

Source: https://exaly.com/author-pdf/8284216/publications.pdf Version: 2024-02-01



#	Article	IF	CITATIONS
1	Burial rates during prograde metamorphism of an ultra-high-pressure terrane: an example from Lago di Cignana, western Alps, Italy. Earth and Planetary Science Letters, 2003, 215, 57-72.	1.8	291
2	Rapid exhumation of the Zermatt-Saas ophiolite deduced from high-precision SmNd and RbSr geochronology. Earth and Planetary Science Letters, 1999, 171, 425-438.	1.8	199
3	Diffusion-limited REE uptake by eclogite garnets and its consequences for Lu–Hf and Sm–Nd geochronology. Contributions To Mineralogy and Petrology, 2006, 152, 703-720.	1.2	194
4	Intercrystalline stable isotope diffusion: a fast grain boundary model. Contributions To Mineralogy and Petrology, 1992, 112, 543-557.	1.2	183
5	A model for coupled fluid-flow and mixed-volatile mineral reactions with applications to regional metamorphism. Contributions To Mineralogy and Petrology, 1991, 106, 273-285.	1.2	143
6	A new look at stable isotope thermometry. Geochimica Et Cosmochimica Acta, 1993, 57, 2571-2583.	1.6	133
7	Time resolved construction of a bimodal laccolith (Torres del Paine, Patagonia). Earth and Planetary Science Letters, 2012, 325-326, 85-92.	1.8	116
8	A least-squares approach to mass transport calculations using the isocon method. Economic Geology, 1995, 90, 1261-1270.	1.8	96
9	Partial Melting and Assimilation of Dolomitic Xenoliths by Mafic Magma: the loko-Dovyren Intrusion (North Baikal Region, Russia). Journal of Petrology, 2002, 43, 2049-2074.	1.1	90
10	7. Stable Isotope Transport and Contact Metamorphic Fluid Flow. , 2001, , 415-468.		81
11	Two-Stage, Extreme Albitization of A-type Granites from Rajasthan, NW India. Journal of Petrology, 2012, 53, 919-948.	1.1	81
12	Coupling of oceanic and continental crust during Eocene eclogite-facies metamorphism: evidence from the Monte Rosa nappe, western Alps. Contributions To Mineralogy and Petrology, 2006, 153, 139-157.	1.2	70
13	The duration of prograde garnet crystallization in the UHP eclogites at Lago di Cignana, Italy. Earth and Planetary Science Letters, 2009, 287, 402-411.	1.8	51
14	One- and two-dimensional models of fluid flow and stable isotope exchange at an outcrop in the Adamello contact aureole, Southern Alps, Italy. American Mineralogist, 1995, 80, 1004-1019.	0.9	51
15	Experimental determination of melt interconnectivity and electrical conductivity in the upper mantle. Earth and Planetary Science Letters, 2017, 463, 286-297.	1.8	44
16	Metastable prograde mineral reactions in contact aureoles. Geology, 2004, 32, 821.	2.0	40
17	Rb–Sr ages from phengite inclusions in garnets from high pressure rocks of the Swiss Western Alps. Earth and Planetary Science Letters, 2014, 395, 205-216.	1.8	39
18	Petrologic and stable isotopic studies of a fossil hydrothermal system in ultramafic environment (Chenaillet ophicalcites, Western Alps, France): Processes of carbonate cementation. Lithos, 2017, 294-295, 319-338.	0.6	39

#	Article	IF	CITATIONS
19	Heterogeneous melt and hypersaline liquid inclusions in shallow porphyry type mineralization as markers of the magmatic-hydrothermal transition (Cerro de Pasco district, Peru). Chemical Geology, 2016, 447, 93-116.	1.4	38
20	Evidence for cavity-dwelling microbial life in 3.22 Ga tidal deposits. Geology, 2016, 44, 51-54.	2.0	38
21	Convective fluid flow through heterogeneous country rocks during contact metamorphism. Journal of Geophysical Research, 1998, 103, 23983-24003.	3.3	35
22	Stochastic permeability models of fluid flow during contact metamorphism. Geology, 1995, 23, 945.	2.0	31
23	High-resolution 3D analyses of the shape and internal constituents of small volcanic ash particles: The contribution of SEM micro-computed tomography (SEM micro-CT). Journal of Volcanology and Geothermal Research, 2015, 293, 1-12.	0.8	31
24	Quartz Reference Materials for Oxygen Isotope Analysis by <scp>SIMS</scp> . Geostandards and Geoanalytical Research, 2017, 41, 69-75.	1.7	30
25	Estimation of a maximum Lu diffusion rate in a natural eclogite garnet. Swiss Journal of Geosciences, 2008, 101, 637-650.	0.5	28
26	Nucleation-dominated crystallization of forsterite in the Ubehebe Peak contact aureole, California. Geology, 1997, 25, 823.	2.0	27
27	Low melting temperature for calcite at 1000 bars on the join CaCO ₃ â€H ₂ O – some geological implications. Terra Nova, 2015, 27, 364-369.	0.9	27
28	Mineralized breccia clasts: a window into hidden porphyry-type mineralization underlying the epithermal polymetallic deposit of Cerro de Pasco (Peru). Mineralium Deposita, 2018, 53, 919-946.	1.7	26
29	SIMS chlorine isotope analyses in melt inclusions from arc settings. Chemical Geology, 2017, 449, 112-122.	1.4	25
30	Weekly to monthly time scale of melt inclusion entrapment prior to eruption recorded by phosphorus distribution in olivine from mid-ocean ridges. Geology, 2017, 45, 1059-1062.	2.0	25
31	The oxygen isotope anatomy of a slowly cooled metamorphic rock. American Mineralogist, 1995, 80, 757-764.	0.9	23
32	Solubility of the assemblage albite+K-feldspar+andalusite+quartz in supercritical aqueous chloride solutions at 650 ŰC and 2 kbar. Chemical Geology, 2003, 200, 377-393.	1.4	23
33	Short magmatic residence times of quartz phenocrysts in Patagonian rhyolites associated with Gondwana breakup. Geology, 2016, 44, 67-70.	2.0	23
34	Measurement of Volume Change and Mass Transfer During Serpentinization: Insights From the Oman Drilling Project. Journal of Geophysical Research: Solid Earth, 2020, 125, e2019JB018877.	1.4	23
35	Fluid mixing as primary trigger for cassiterite deposition: Evidence from in situ l´180-l´11B analysis of tourmaline from the world-class San Rafael tin (-copper) deposit, Peru. Earth and Planetary Science Letters, 2021, 563, 116889.	1.8	23
36	Experimental study on the solubility of the "model―pelite mineral assemblage albite + K-feldspar + andalusite + quartz in supercritical chloride-rich aqueous solutions at 0.2 GPa and 600°C. Geochimica Et Cosmochimica Acta, 2001, 65, 4493-4507.	1.6	22

#	Article	IF	CITATIONS
37	Source and fractionation controls on subduction-related plutons and dike swarms in southern Patagonia (Torres del Paine area) and the low Nb/Ta of upper crustal igneous rocks. Contributions To Mineralogy and Petrology, 2018, 173, 38.	1.2	22
38	The role of the antigorite + brucite to olivine reaction in subducted serpentinites (Zermatt,) Tj ETQq0 0	0 rgBT ∕Ov	rerlock 10 Tf
39	Provenance of Jurassic Tethyan sediments in the HP/UHP Zermatt-Saas ophiolite, western Alps. Bulletin of the Geological Society of America, 2005, 117, 530.	1.6	21
40	Experimental determination of anorthite solubility and calcium speciation in supercritical chloride solutions at 2 kb from 400 to 600°C. Geochimica Et Cosmochimica Acta, 1995, 59, 1539-1549.	1.6	20
41	Modelling mid-crustal migmatite terrains as feeder zones for granite plutons: the competing dynamics of melt transfer by bulk versus porous flow. Earth and Environmental Science Transactions of the Royal Society of Edinburgh, 2004, 95, 49-58.	0.3	20
42	An observational and thermodynamic investigation of carbonate partial melting. Earth and Planetary Science Letters, 2015, 409, 147-156.	1.8	20
43	Forward modeling of the effects of mixed volatile reaction, volume diffusion, and formation of submicroscopic exsolution lamellae on calcite-dolomite thermometry. American Mineralogist, 2008, 93, 1245-1259.	0.9	16
44	Oxygen isotope speedometry in granulite facies garnet recording fluid/melt–rock interaction (SÃ,r) Tj ETQq0 0	0 rgBT /Ov	verlock 10 Tf
45	Stacking fault-enhanced argon diffusion in naturally deformed muscovite. Geological Society Special Publication, 2003, 220, 249-260.	0.8	15
46	Growth mechanism of snowball garnets from the Lukmanier Pass area (Central Alps, Switzerland): a combined ?CT/EPMA/EBSD study. Terra Nova, 2007, 19, 240-244.	0.9	15
47	Constraining magmatic fluxes through thermal modelling of contact metamorphism. Geological Society Special Publication, 2015, 422, 41-56.	0.8	15
48	Cosmicâ€ray exposure ages of chondrules. Meteoritics and Planetary Science, 2016, 51, 1256-1267.	0.7	14
49	Evaluation of potential monazite reference materials for oxygen isotope analyses by SIMS and laser assisted fluorination. Chemical Geology, 2017, 450, 199-209.	1.4	13
50	Multi fluid-flow record during episodic mode I opening: A microstructural and SIMS study (Cotiella) Tj ETQq0 0 0	rgBT /Over	rlock 10 Tf 5

51	Origin of Monte Rosa whiteschist from in-situ tourmaline and quartz oxygen isotope analysis by SIMS using new tourmaline reference materials. American Mineralogist, 2019, 104, 1503-1520.	0.9	13
52	Tracing of Cl input into the sub-arc mantle through the combined analysis of B, O and Cl isotopes in melt inclusions. Earth and Planetary Science Letters, 2019, 507, 30-39.	1.8	13
53	A Method for Secondary Ion Mass Spectrometry Measurement of Lithium Isotopes in Garnet: The Utility of Glass Reference Materials. Geostandards and Geoanalytical Research, 2021, 45, 477-499.	1.7	13
54	Timing and thermal evolution of fold-and-thrust belt formation in the Ultima Esperanza District, 51°S Chile: Constraints from K-Ar dating and illite characterization. Bulletin of the Geological Society of America, 2018, 130, 975-998.	1.6	12

#	Article	IF	CITATIONS
55	Reactive fluid infiltration along fractures: Textural observations coupled to in-situ isotopic analyses. Earth and Planetary Science Letters, 2019, 519, 264-273.	1.8	11
56	Porosity and Permeability of Carbonate Rocks During Contact Metamorphism. , 1997, , 83-98.		11
57	Oxygen isotope disequilibrium during serpentinite dehydration. Terra Nova, 2019, 31, 94-101.	0.9	10
58	New U-Pb zircon data and constraints on the age and mode of migmatization in the Aar massif, Central Alps. European Journal of Mineralogy, 2000, 12, 1245-1260.	0.4	10
59	Metamorphic transformation rate over large spatial and temporal scales constrained by geophysical data and coupled modelling. Journal of Metamorphic Geology, 2021, 39, 1131-1143.	1.6	9
60	Fast and pervasive diagenetic isotope exchange in foraminifera tests is species-dependent. Nature Communications, 2022, 13, 113.	5.8	9
61	Silica-undersaturated reaction zones at a crust–mantle interface in the Highland Complex, Sri Lanka: Mass transfer and melt infiltration during high-temperature metasomatism. Lithos, 2017, 284-285, 237-256.	0.6	8
62	Development and Reâ€Evaluation of Tourmaline Reference Materials for In Situ Measurement of Boron δ Values by Secondary Ion Mass Spectrometry. Geostandards and Geoanalytical Research, 2020, 44, 593-615.	1.7	8
63	Tracking fluid mixing in epithermal deposits – Insights from in-situ δ18O and trace element composition of hydrothermal quartz from the giant Cerro de Pasco polymetallic deposit, Peru. Chemical Geology, 2021, 576, 120277.	1.4	8
64	Whiteschist genesis through metasomatism and metamorphism in the Monte Rosa nappe (Western) Tj ETQq0 C	0 rgBT /C 1:2	verlock 10 Tf
65	Peak Alpine metamorphic conditions from stauroliteâ€bearing metapelites in the Monte Rosa nappe (Central European Alps) and geodynamic implications. Journal of Metamorphic Geology, 2021, 39, 897-917.	1.6	7
66	Modelling changes in stable isotope compositions of minerals during net transfer reactions in a contact aureole: Wollastonite growth at the northern Hunter Mountain Batholith (Death Valley) Tj ETQq0 0 0 rg	BT 1 @verlo	ck@10 Tf 50 2
67	Protracted storage of <scp>CR</scp> chondrules in a region of the disk transparent to galactic cosmic rays. Meteoritics and Planetary Science, 2017, 52, 2166-2177.	0.7	5
68	The zircon Hf isotope archive of rapidly changing mantle sources in the south Patagonian retro-arc. Bulletin of the Geological Society of America, 2019, 131, 587-608.	1.6	5
69	Carbonatitic dykes during Pangaea transtension (Pelagonian Zone, Greece). Lithos, 2018, 302-303, 329-340.	0.6	4
70	Accurate Measurements of H ₂ 0, F and Cl Contents in Biotite Using Secondary Ion Mass Spectrometry. Geostandards and Geoanalytical Research, 2018, 42, 523-537.	1.7	4
71	Grain scale processes recorded by oxygen isotopes in olivine-hosted melt inclusions from two MORB samples. Chemical Geology, 2019, 511, 11-20.	1.4	4
72	Mineral Dissolution and Precipitation Under Stress: Model Formulation and Application to Metamorphic Reactions. Geochemistry, Geophysics, Geosystems, 2021, 22, e2021GC009633.	1.0	4

#	Article	IF	CITATIONS
73	Alpine peak pressure and tectono-metamorphic history of the Monte Rosa nappe: evidence from the cirque du VA©raz, upper Ayas valley, Italy. Swiss Journal of Geosciences, 2021, 114, 20.	0.5	2
74	Modelling mid-crustal migmatite terrains as feeder zones for granite plutons: the competing dynamics of melt transfer by bulk versus porous flow. , 2004, , .		1
75	Interplay between fluid circulation and Alpine metamorphism in the Monte Rosa whiteschist from white mica and quartz in situ oxygen isotope analysis by SIMS. American Mineralogist, 2022, 107, 860-872.	0.9	1
76	Limited channelized fluid infiltration in the Torres del Paine contact aureole. American Mineralogist, 2021, 106, 1453-1469.	0.9	1
77	Reply to: Comment on "Solubility of the Assemblage Albite+K-Feldspar+Andalusite+Quartz in Supercritical Aqueous Chloride Solutions at 650 °C and 2 kbar―by D.J. Wesolowski. Chemical Geology, 2004, 211, 179-180.	1.4	0